

Diffusion-weighted MRI Before and After Robotic Radiosurgery (Cyberknife®) in Primary and Secondary Liver Malignancies: A Pilot Study

www.tcert.org
DOI: 10.7785/tert.2012.500408

The purpose of this study was to evaluate the role of diffusion-weighted MR imaging (DW-MRI) in the assessment of treatment response of primary or secondary liver malignancies after stereotactic radiosurgery (SRS) using robotic radiosurgery. All patients who underwent SRS therapy for hepatic malignancies who had pre- and post-interventional MR examinations including DW-MRI at our hospital between 02/2010 and 02/2012 were included. A retrospective analysis of the institutional imaging database identified 13 patients (4 men, 9 women, mean age: 66 years) with a total of 14 primary or secondary liver malignancies. Criteria of tumor response to treatment were a decrease in size and/or loss of contrast enhancement as assessed with respect to RECIST criteria. Mean apparent diffusion coefficient (ADC) values for normal liver parenchyma and hepatic masses in each MR examination were calculated and compared using two-tailed, paired *t*-test with a significance level of 0.05. Mean ADC values of liver malignancies were $1.10 \pm 0.30 \times 10^{-3} \text{ mm}^2/\text{s}$, $1.48 \pm 0.35 \times 10^{-3} \text{ mm}^2/\text{s}$ and $1.56 \pm 0.40 \times 10^{-3} \text{ mm}^2/\text{s}$ on pre-interventional, the first post-interventional, and the second post-interventional DW-MRI. There was a significant increase of ADC values between the pre-interventional examination and the first and second post-interventional follow-up exams ($p < 0.01$ and $p = 0.01$, respectively). However, there was no statistical difference between the ADC values of the first and second post-interventional MRI. ADC values of normal liver parenchyma did not show significant changes in ADC values during pre- and post-interventional MRI. ADC measurements may allow the evaluation of response to treatment of hepatic malignancies by SRS. ADC values of liver malignancies increase significantly after SRS treatment.

Key words: Diffusion-weighted MRI; Robotic radiosurgery; Liver.

Introduction

Hepatocellular carcinoma (HCC) and secondary liver metastases comprise a large proportion of malignancies diagnosed in the United States and worldwide (1). Surgical resection is currently the accepted standard treatment method for potential cure, demonstrating benefit in overall survival time in primary and secondary liver malignancies (2-4). Due to the presence of metastatic disease and/or

Christine Schmid-Tannwald,
M.D.^{1*†}
Frederik F. Strobl, M.D.^{1†}
Daniel Theisen, M.D.¹
Alexander Muacevic, M.D.²
Sebastian Stintzing, M.D.³
Maximilian F. Reiser, M.D.¹
Christoph G. Trumm, M.D.¹

¹Department of Clinical Radiology,
University Hospital Grosshadern,
LMU Munich, Munich, Germany

²European Cyberknife Center Munich,
Munich, Germany

³Department of Medical Oncology
and Comprehensive Cancer Center,
Klinikum Grosshadern, LMU,
Munich, Germany

[†]These authors contributed equally to
this work and share first authorship.

Mailing list for each institution:

¹christine.schmid-tannwald@med
.uni-muenchen.de

²sebastian.stintzing@med
.uni-muenchen.de

³Alexander.Muacevic@cyber-knife.net

Abbreviations: ADC: Apparent Diffusion Coefficient; CT: Computed Tomography; DWI: Diffusion Weighted Imaging; EPI: Echoplanar Imaging; FLL: Focal Liver Lesion; GD-EOB-DTPA: Gadolinium Ethoxybenzyl Diethylenetriamine Penta-acetic Acid; HCC: Hepatocellular Carcinoma; LINAC: Compact Linear Accelerator; MRI: Magnetic Resonance Imaging; MWA: Microwave Ablation; PET-CT: Positron Emission Tomography-Computed Tomography; RECIST: Response Criteria in Solid Tumors; RFA: Radiofrequency Ablation; ROI: Region of Interest; RT: Radiotherapy; SBRT: Stereotactic Body Radiation Therapy; SRS: Stereotactic Radiosurgery; VOI: Volume of Interest.

*Corresponding author:
Christine Schmid-Tannwald, M.D.
Phone: +49 89 7095 0
E-mail: christine.schmid-tannwald@med
.uni-muenchen.de

cardiovascular, pulmonary, or hepatic comorbidities, curative surgery is only pursued in a minority of patients (5-7). Therefore, less invasive procedures are needed to offer treatment options for non-surgical candidates. The most frequently utilized alternatives to surgical resection are thermal ablation procedures such as radiofrequency ablation (RFA), microwave ablation (MWA), and laser-induced thermal therapy (LITT) (8-10).

However, thermoablative procedures have limitations. For example, the maximum diameter of treatable hepatic malignancies is currently limited to 3 cm. Furthermore, malignancies in the vicinity of large blood vessels (that may impede complete tumor ablation due to heat-sink effects), bile ducts, or neighboring organs may not be amenable to thermoablative procedures (11). Therefore, radiation therapy techniques have been increasingly used to treat hepatic malignancies in the recent past. Stereotactic body radiation therapy (SBRT) using fewer fractions and more localized treatment approaches has shown promising treatment effects in cases that are not otherwise amenable to other treatments (12, 13). The Cyberknife® system is a robotic radiation device characterized by a compact linear accelerator (LINAC) mounted on a six-axis robotic manipulator. This system configuration facilitates the tracking of a respiratory motion dependent, moving target like a liver tumor, allowing real time tracking during the treatment cycle. The system also has the capability of applying a local ablative dose of radiation in just one treatment session for selected liver lesions (14, 15). Recently a matched-pair analysis comparing RFA and Cyberknife® in colorectal liver metastases showed a better local progression free survival time in favor for the Cyberknife® treatment group without a difference in overall survival (16).

Diffusion-weighted imaging (DW-MRI) is increasingly used in the abdomen, especially in the liver for detection and characterization of focal liver lesions (FLL). Malignant lesions generally show restricted diffusion with high signal on high *b*-value diffusion-weighted images and low ADC values. ADC measurements may also be useful for a quantitative analysis of focal liver lesions, since ADC values of malignant lesions are lower than those of the normal liver and benign liver lesions. Recent studies have aimed to define ADC thresholds allowing differentiation between benign and malignant lesions (17).

Beyond the advantages of DW-MRI regarding the detection and characterization of FLL, DW-MRI can provide valuable information in the evaluation of tumor response to treatment such as radiation therapy, chemotherapy and local ablation (18-25). Shortly following transarterial chemoembolization (21) and radioembolization (23), ADC values of hepatocellular carcinoma are increased over

pre-operative values. These are followed by a substantial further increase of ADC values due to tumor necrosis and cystic changes (25).

To the best of our knowledge, no previous reports have evaluated the use of DW-MRI in the assessment of the response of primary or secondary liver malignancies to stereotactic radiosurgery (SRS) treatment. Therefore, the purpose of this study was to determine whether tumor ADC values increase after SRS treatment and to evaluate the role of DW-MRI in the assessment of treatment response.

Material and Methods

Patients

The study endorsed was performed according to the principles of the Declaration of Helsinki and subsequent amendments (26). Approval of the local institutional ethics board was waived since all studies were performed within the framework of established clinical diagnostic workup. Informed consent to the MRI examination and robotic radiosurgery treatment was obtained from all patients prior to the procedure.

Consecutive patients (*n* = 41) who received SRS for primary/or secondary liver malignancies and had one pre-interventional and one post-interventional MRI performed at our institution between 02/2010 and 02/2012 were included. A retrospective analysis of the institutional imaging database identified 13 such patients (9 female, 4 male; mean age: 66 years ± 7.3). Patients not fulfilling these criteria were excluded from this study.

MR Imaging

All patients were positioned supine in a 1.5T MRI system (Magnetom Avanto, Magnetom Aera Siemens Healthcare, Erlangen, Germany). A phased-array-coil was utilized for signal reception. The routine MRI protocol included an unenhanced T1w 2D gradient echo (GRE) sequence in- and out-of-phase, a navigator gated half-fourier acquisition single-shot T2w FSE (HASTE) sequence without fat suppression, and a T1w 3D GRE sequence with fat suppression (VIBE) before contrast administration. Dynamic contrast enhanced imaging was performed after intravenous injection of 0.025 mmol/kg gadolinium ethoxybenzyl diethylenetriamine penta-acetic acid (Gd-EOB-DTPA, Bayer Healthcare, Berlin, Germany) at a rate of 1-2 ml/s followed by a saline chaser. Images were acquired in the arterial, portal venous (60-80 s post-injection), and late venous phases (120-140 s post-injection) with the 3D VIBE sequence. Hepatobiliary phase images were acquired 20 min following contrast administration. During the time interval between

Table I
Sequence parameters (Magnetom Aera and Magnetom Avanto).

Sequence and parameters	T2w Single shot fast spin echo (SSFSE)	DW-MRI	T1w 3D Gradient-echo, fat saturated (GRE FS) Pre- & Dynamic Post-contrast
Parallel imaging	2	2	2
Fat saturation	No	Yes	Yes
Respiratory state	Free-breathing	Respiratory gated	Inspiration
TR (ms)	800	2800 (2300)	3.35
TE (ms)	84 (54)	66 (70)	1.19
TI (ms)	–	–	–
FA (deg)	180	180	15
FOV	380 mm 100% (380 mm 75%)	400 mm 75% (400 mm 65%)	360 mm 75% (400 mm 75%)
Matrix	320 × 320 (320 × 189)	192 × 130 (192 × 113)	256 × 154
Slice orientation	Transverse	Transverse	Transverse
Slice thickness (mm)	6 mm	6 mm	3 mm
Slice gap (mm)	0.6 mm	0.6 mm	No gap
No. of slices	35	30	64 (56)
Bandwidth (Hz/pixel)	710 (446)	1370	450
<i>k</i> -space sampling	Linear	All <i>k</i> -space lines are measured in one TR	Line by line, time to center 6.5 s
Acquisition time	***	***	21 s (19s)
<i>b</i> -value (s/mm ²)	–	50, 800	–

***Acquisition time is dependent on the individual patient's respiratory rate.

Parameters of Magnetom Avanto 1.5 T deviating from those of the Magnetom Aera are delineated parenthetically in bold.

the late venous and hepatobiliary phase images, high-resolution navigator-gated T2w FSE images with fat saturation and diffusion weighted images were acquired. Diffusion weighted imaging (DWI) was performed with a single-shot SE echoplanar imaging (EPI) sequence with *b*-values of 50 and 800 s/mm². Detailed sequence parameters are provided in Table I.

Robotic Radiosurgery

The treatment of liver malignancies was performed with the Cyberknife® robotic radiosurgery system (Accuray, Sunnyvale, CA). This is the only radiation technology currently available that is capable of real-time tumor tracking, thus facilitating evaluation of malignancies that move with respiration. Before treatment, fiducial gold markers were implanted percutaneously under CT-fluoroscopic guidance by an experienced interventional radiologist. These markers are required to provide motion tracking of lesions which are affected by respiratory motion (27). The 3D target volume was identified on both contrast-enhanced CT (arterial and portal venous phase) and MRI scans which were fused for optimal target definition. A safety margin of 6 mm was added to the tumor diameter in all three dimensions to account for microscopic tumor spread. 26 Gy were applied in one fraction to the 70% isodose line resulting in a maximum tumor dose of over 30 Gy in the center of the lesion.

Radiation was performed with a 6 MV compact LINAC mounted on a six-axis robotic manipulator. The position of the LINAC was corrected in real time during the treatment on the basis of the position of the gold markers detected by two X-ray detectors arranged orthogonally to each other and infrared markers on the patient's chest tracked continuously with external cameras. This allowed for compensation of changes in the position of the irradiated volume caused by breathing. The radiation beam itself could be directed from a multitude of angles around the patient (*i.e.* more than 1500 directions).

Image Evaluation

All MRI data were reviewed by two radiologists in consensus (Observer 1 and 2 with 7 and 8 years experience in abdominal MRI). On each MR examination the number and location (liver segment) of each lesion treated by robotic radiosurgery were recorded.

Response to Treatment: The size of each lesion was measured on each T1-weighted post-contrast image of the liver on the pre-intervention as well as the first and second post-intervention MRI's. The evaluation of treatment response was based on the vascularity and on the size of the lesion on follow-up imaging.

ADC Measurements: ADC maps were generated from DW-MR images. ADC values of normal liver parenchyma and of the hepatic malignancies were calculated. For ADC measurements of normal liver parenchyma, a region of interest (ROI) was placed in the normal liver on the ADC maps. This ROI was drawn as large as possible while avoiding intrahepatic vessels, bile ducts, and regions of motion artifact. For ADC measurements of the lesions, freehand ROIs were drawn around the lesions using SyngoVia (Siemens Healthcare, Forchheim, Germany). The ROI drawing was performed in consensus by the two observers. First, freehand ROIs were drawn over the entire tumor as visualized on the image with the greatest diameter on T2-weighted and diffusion-weighted images (b -value of $800 \text{ mm}^2/\text{s}$). Then, this ROI was copied and pasted into the same slice of the ADC map. The corresponding ADC values were used for statistical analysis.

Reference Standard: Clinical and surgical records were collected by a third radiologist with 5 years of experience in body MRI. Following the image evaluation sessions, the three radiologists reviewed all MRI examinations, further follow-up cross-sectional imaging (CT, PET-CT), and clinical records in order to establish a consensus diagnosis.

Statistical Analysis

For statistical analysis of baseline patient characteristics and changes of ADC over time, standard statistical software was utilized (SPSS software, Version 18, IBM, Seattle, WA). Mean ADC values for normal liver parenchyma and hepatic lesions of each MRI examination were calculated and compared using a two-tailed, paired t -test with a significance level of 0.05.

Results

Reference Standard

The consensus review of T2w, DW-MRI, CE-T1w images along with clinical and surgical records found a total of 14 hepatic liver malignancies which were treated by SRS: 3 were HCC, 11 were metastases. All fourteen malignancies were pathologically proven. One lesion was located in liver segment 2 and 6, respectively. Two lesions were located in segment 4b, 5 and 7; three malignancies were located in segment 4a and 6, respectively. Baseline patient and lesion characteristics are given in Table II.

All patients had undergone MR imaging, including DWI, with a mean of 24.6 ± 14.8 days (range, 2-59) before SRS treatment. The first post-procedural MR examination was carried out in all 13 patients with a mean of 77.6 ± 28.3 days (range, 15-119) after SRS. The second post-procedural

Table II
Patient characteristics.

Age (MV \pm SD)	66.3 \pm 7.4
Gender	
Male	6 (46.2%)
Female	7 (53.8%)
Total	13
Tumor Type	
HCC	3 (21.4%)
Colorectal metastasis	7 (50%)
NET metastasis	1 (7.1%)
CCC metastasis	1 (7.1%)
Breast metastasis	1 (7.1%)
Pancreas metastasis	1 (7.1%)

MR examination was obtained in 12 patients at a mean of 238.4 ± 129.4 days (range, 142-609) following SRS.

Response of Treatment: 13 of 14 treated lesions showed a decrease in size. The mean size of the malignancies was 3.2 ± 1.7 cm on the pre-interventional MR imaging, 2.4 ± 1.3 cm on the post-interventional imaging, and 2.2 ± 0.9 cm on the second post-interventional imaging. In total, there was a decrease in size of more than 30% (mean decrease 68.75%), which fulfils the criteria of partial response with respect to RECIST criteria (28).

One of 14 lesions did not show a decrease in size. However, on the dynamic MRI and in the follow-up imaging there was no further detectable vascularity of the lesion. The other 13 lesions still demonstrated enhancement on post-interventional MR images.

ADC Measurements: Mean ADC values of the normal liver parenchyma were $1.19 \pm 0.19 \times 10^{-3} \text{ mm}^2/\text{s}$, $1.16 \pm 0.21 \times 10^{-3} \text{ mm}^2/\text{s}$, and $1.16 \pm 0.16 \times 10^{-3} \text{ mm}^2/\text{s}$ on pre-interventional, first post-interventional, and second post-interventional DW-MRI, respectively. There were no statistically significant differences in normal hepatic parenchymal ADC values between these three examinations ($p > 0.05$).

Mean ADC values of liver malignancies were $1.10 \pm 0.30 \times 10^{-3} \text{ mm}^2/\text{s}$, $1.48 \pm 0.35 \times 10^{-3} \text{ mm}^2/\text{s}$, and $1.56 \pm 0.40 \times 10^{-3} \text{ mm}^2/\text{s}$ on the pre-interventional, first post-interventional, and second post-interventional DW-MRI, respectively. There was a statistically significant increase of ADC values between the pre-interventional examination and the first and second post-interventional follow-up examinations ($p < 0.01$ and $p = 0.01$, respectively) (Figures 1 and 2). However, there was no significant difference between ADC values of liver malignancies on the first and the second follow-up MR examination ($p = 0.57$). ADC values are given in Table III.

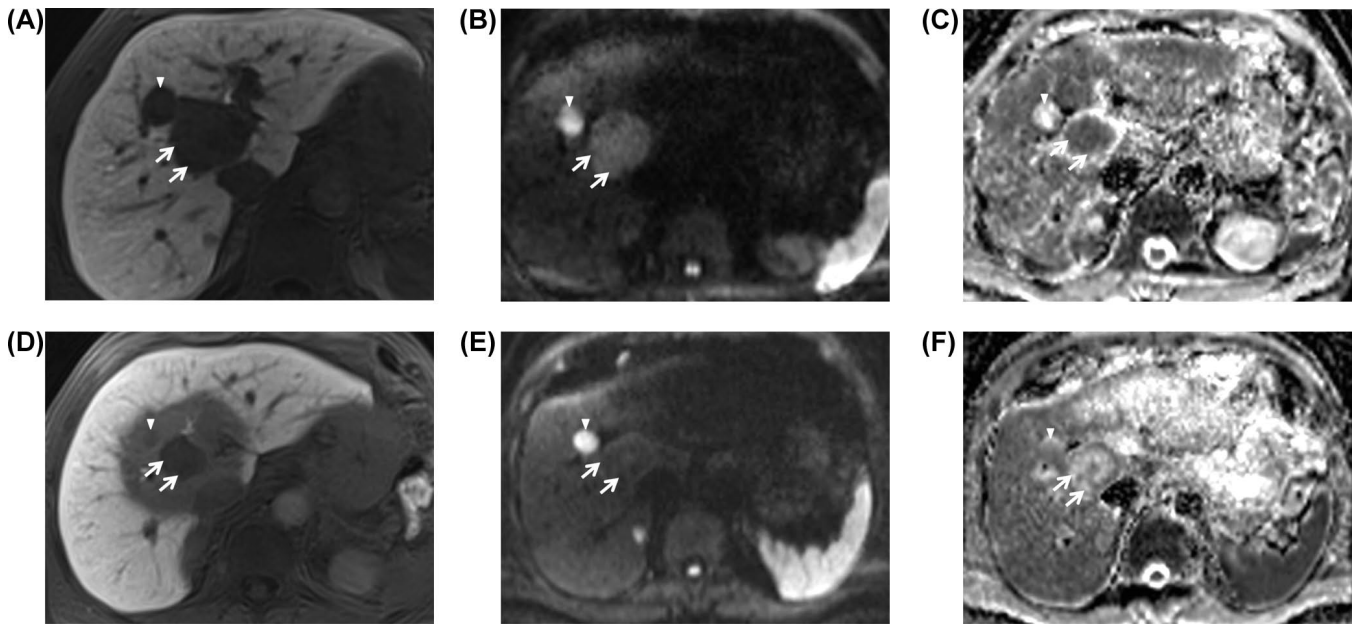


Figure 1: 67 year old male with hepatocellular carcinoma. The pre-interventional axial contrast-enhanced T1-weighted image (hepatobiliary phase) (A) shows a hypointense lesion (arrows) compatible with hepatocellular carcinoma (HCC). In addition to this lesion (arrow head) a smaller second lesion was identified and diagnosed as a hemangioma. The HCC shows restricted diffusion with high signal on axial DW-MR image $b = 800 \text{ s/mm}^2$ (B) and dark signal on ADC map (C). The pre-interventional ADC value of the HCC was $0.77 \times 10^{-3} \text{ mm}^2/\text{s}$. After Cyberknife therapy, the HCC exhibited a decrease in size with perilesional edema on the axial contrast-enhanced T1-weighted image (hepatobiliary phase) (D). On the axial DW-MR image $b = 800 \text{ s/mm}^2$ (E), the HCC demonstrated isointense signal to liver and predominantly hyperintense signal with a hypointense rim on the ADC map (F) indicating less restricted diffusion compared to the pre-interventional image. The post-interventional ADC value of the HCC was $1.58 \times 10^{-3} \text{ mm}^2/\text{s}$.

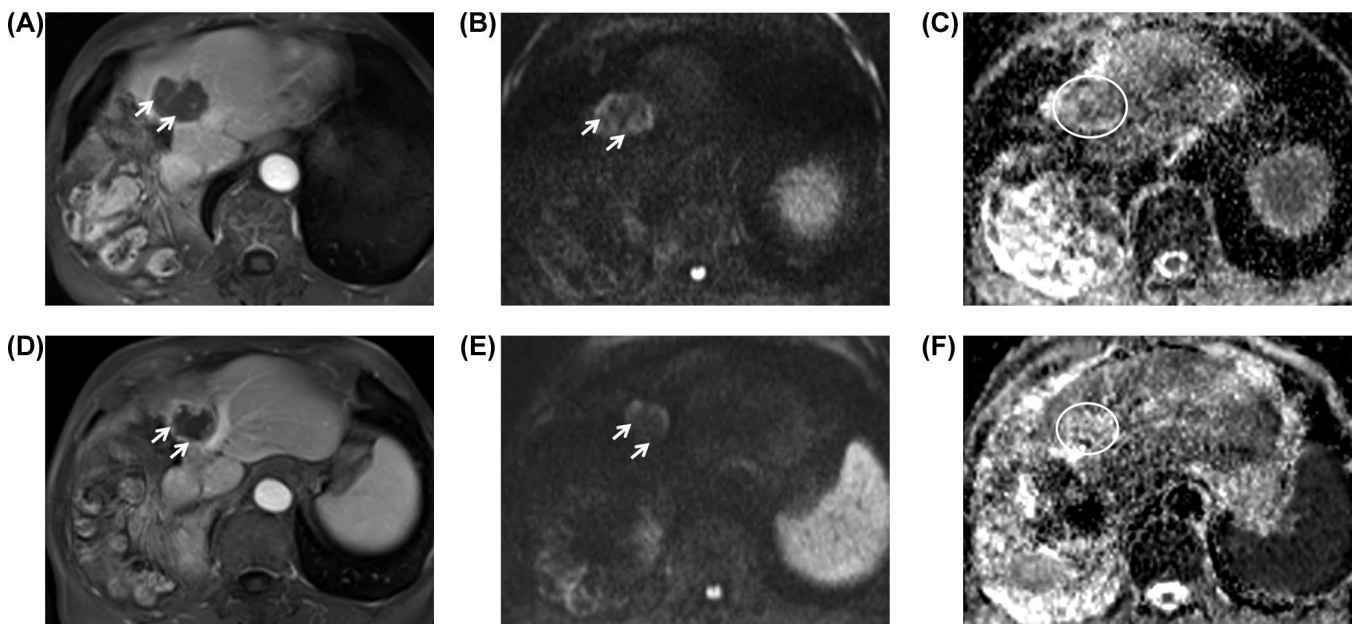


Figure 2: 70 year old female with rectal adenocarcinoma metastases to the liver. The pre-interventional axial contrast-enhanced T1-weighted image (portal-venous phase) (A) shows a hypointense lesion with rim enhancement (arrows) compatible with a hypovascular metastasis. The metastasis shows restricted diffusion with high signal on axial DW-MR image $b = 800 \text{ s/mm}^2$ (B) and intermediate to dark signal on ADC map (C). The pre-interventional ADC value of the metastasis was $1.20 \times 10^{-3} \text{ mm}^2/\text{s}$. After Cyberknife therapy, the metastasis decreased in the size from 4.2cm to 3.6cm on the axial contrast-enhanced T1-weighted image (liver-specific phase) (D). The metastasis showed a loss of signal compared to the pre-interventional DW-MR image $b = 800 \text{ s/mm}^2$ (E), and predominantly hyperintense signal on the ADC map (F) indicating loss of restricted diffusion compared to the pre-interventional image. The post-interventional ADC value of the HCC was $1.61 \times 10^{-3} \text{ mm}^2/\text{s}$.

Table III
Results of the ADC analysis (Mean Value \pm Standard Deviation).

Measurement 1: Before SRS	Measurement 2: First follow-up after SRS	Measurement 3: Second follow-up after SRS
1.10 \pm 0.30	1.48 \pm 0.35	1.56 \pm 0.40
<i>p</i> -value between measurement 1 and 2: <0.01		<i>p</i> -value between measurement 2 and 3: 0.57
<i>p</i> -value between measurement 1 and 3: <0.01		

Discussion

The goal of this study was to investigate ADC value changes in malignancies treated by robotic radiosurgery. Our results show that the mean ADC values of liver malignancies increase significantly after SRS treatment. Therefore DW-MRI may be a useful adjunct to evaluate the tumor response of liver lesions treated by SRS. Robotic stereotactic radiotherapy such as robotic radiosurgery is a relatively new treatment option for primary or secondary liver malignancies, and is particularly useful when standard treatment options such as surgery or local ablative therapies are not feasible. Good response rates and tolerance in terms of hepatic function have been reported (16, 29-31).

The early determination of response to local therapies such as SRS is crucial with respect to evaluation of the treatment success. Early determination of treatment response helps minimize the unnecessary use of chemotherapeutic agents, and aids in planning reintervention or additional treatments if needed. This allows for improved management of the disease, and yields important information regarding prognosis and patient quality of life.

Assessment of response to an anti-cancer treatment is usually based on tumor size on cross-sectional imaging. The Response Evaluation Criteria in Solid Malignancies (RECIST) criteria is the most commonly used evaluation tool (28, 32, 33). However, the exact lesion size may be difficult to measure due to wide interobserver variability in estimating the exact boundary of the lesion (33). In liver tumors, especially in HCC, it can take several months before there is significant change in tumor size following local therapy (34). Furthermore, necrotic or fibrotic tumor changes may not be accurately detected or differentiated from residual tumor by imaging, resulting in underestimation of treatment response (33). This is especially the case after local or targeted tumor therapy (35, 36). After chemoembolization, there seems to be a discrepancy between the reduction in tumor size seen on imaging and the degree of necrosis at histopathology (21, 37).

DW-MRI is based on the motion of water molecules in the extracellular space, and provides visualization of

Brownian molecular motion (18). There is a negative correlation between the degree of restriction of water diffusion in biologic tissue and the tissue cellularity and integrity of cell membranes (38-40). Therefore, DW-MRI provides qualitative and quantitative information regarding tissue cellularity and the integrity of cell membranes. Intralesional cystic or necrotic changes result in less diffusion restriction since water molecules are able to move freely (25, 41). With advances in MR hardware, sequence design, and reconstruction, DW-MRI is increasingly used in the liver not only for detection and characterization of focal liver lesions but also for the monitoring of treatment response of hepatic tumors.

In a study by Kamel *et al.* hepatocellular carcinoma demonstrated a significant increase in ADC values (from $1.5 \times 10^{-3} \text{ mm}^2/\text{s}$ to $1.8 \times 10^{-3} \text{ mm}^2/\text{s}$) after transarterial chemoembolization (21). Although mean ADC values of liver malignancies in our study were lower, we could also nevertheless demonstrate a significant increase in ADC values from $1.10 \times 10^{-3} \text{ mm}^2/\text{s}$ to up to $1.56 \pm 0.40 \times 10^{-3} \text{ mm}^2/\text{s}$ after treatment. In terms of explaining variations between our data and the study of Kamel *et al.*, technical factors such as differences in DW-MR image acquisition technique, the different MR scanners utilized, and the different types of treatment performed could certainly play a role. Anzidei *et al.* similarly found ADC values of colorectal liver metastases to increase significantly after chemotherapy and antiangiogenic treatment (24). Deng *et al.* also demonstrated that ADC values of hepatocellular carcinoma (HCC) increased significantly after Yttrium-90 radioembolization (23). The increase of ADC values may be attributable to therapy-induced necrotic or cystic tumor changes (25).

The therapeutic mechanism of percutaneous (*e.g.* RFA) or transarterial (*e.g.* chemoembolization, radioembolization) treatments mentioned above cannot be directly compared to radiation therapies such as Cyberknife®. This is because SRS does not cause acute necrosis, but results instead in tumor cell death which may last weeks or even months following therapy. These features make early follow up MRI imaging particularly difficult to interpret.

Two studies have evaluated DWI in patients with liver malignancies treated by radiotherapy. The feasibility of using

changes in ADC values as a surrogate for tumor response to radiotherapy was demonstrated by Eccles *et al.* in 11 patients treated with six-fraction conformal liver RT (42). Median ADC in treated tumor volumes of interest (VOI) progressively increased from pre-treatment scans to scans performed during weeks 1 and 2 of RT, to scans performed 1 month following RT. Early increases in mean ADC correlated with a higher radiation dose and an increased likelihood of response. Tumor response to brachytherapy of colorectal liver metastases was assessed by DWI in a study with 30 patients undergoing single-fraction ¹⁹²Ir-high-dose-rate brachytherapy (43). Pre-treatment DWI and post-treatment imaging was performed two days and three months following therapy. Compared with baseline ADC measurements, mean ADC of treated malignancies decreased by 11.4% two days after treatment, but increased by 28.6% three months after the therapy, a finding consistent with our results. These studies indicate that DWI may be able to accurately assess tumor response to conformal radiotherapy and brachytherapy in hepatic cancer.

In addition to CT and MRI, hybrid-modalities such as PET-CT may also serve as methods to evaluate success rates of robotic radiosurgery. PET-CT enables both anatomic and metabolic evaluation of malignancies, allowing comparison of pre- and post-treatment metabolism (44). However to date, no report has been published on the feasibility of PET-CT in the evaluation of robotic radiosurgery treatments in liver malignancies. Thus, we would currently suggest that MRI with DWI is the most suitable imaging modality in the pre-procedural planning and post-procedural follow-up of liver tumors to be treated with robotic radiosurgery.

Our study has several limitations. This was a pilot study to demonstrate feasibility of DW-imaging in the follow-up after Robotic radiosurgery. Therefore we did not analyze the difference between responders and non-responders to the treatment. This would not have been possible due to the relatively small patient cohort. In addition we did not evaluate possible technical artifacts (*e.g.* motion artifacts) or artifacts due to morphologic heterogeneity of the tumor (tumor structure or hemorrhage), and there was no confirmation of post-procedural results through histopathological examinations. This would not have been ethically feasible due to the invasiveness of a liver biopsy. Furthermore the evaluation of the images and the ADC measurements were done in consensus. Additional studies may be useful to assess intra- and inter-observer variability of results.

Further, larger studies with long-term follow-up correlation are necessary to confirm the results herein. However, on the basis of this work, it appears DW-MRI may serve as a useful tool for the follow-up evaluation of local tumor response after SRS of primary and secondary liver malignancies.

Conflict of Interest

There is nothing to disclose.

The authors or authors institutions have no conflicts of interest.

References

1. Soerjomataram, I., Lortet-Tieulent, J., Parkin, D. M., Ferlay, J., Mathers, C., Forman, D., Bray, F. Global burden of cancer in 2008: a systematic analysis of disability-adjusted life-years in 12 world regions. *Lancet* 380, 1840-1850 (2012). DOI: 10.1016/S0140-6736(12)60919-2
2. Shah, S. A., Bromberg, R., Coates, A., Rempel, E., Simunovic, M., Gallinger, S. Survival after liver resection for metastatic colorectal carcinoma in a large population. *Journal of the American College of Surgeons* 205, 676-683 (2007). DOI: 10.1016/j.jamcollsurg.2007.06.283
3. McLoughlin, J. M., Jensen, E. H., Malafa, M. Resection of colorectal liver metastases: current perspectives. *Cancer Control: Journal of the Moffitt Cancer Center* 13, 32-41 (2006). PMID: 16508624
4. de Lope, C. R., Tremosini, S., Forner, A., Reig, M., Bruix, J. Management of HCC. *Journal of Hepatology* 56(Suppl. 1), S75-87 (2012). DOI: 10.1016/S0168-8278(12)60009-9
5. Buchler, P., Pfannschmidt, J., Rudek, B., Dienemann, H., Lehnert, T. Surgical treatment of hepatic and pulmonary metastases from non-colorectal and non-neuroendocrine carcinoma. *Scandinavian Journal of Surgery: SJS: Official Organ for the Finnish Surgical Society and the Scandinavian Surgical Society* 91, 147-154 (2002). PMID: 12164514
6. Yoon, S. S., Tanabe, K. K. Surgical treatment and other regional treatments for colorectal cancer liver metastases. *The Oncologist* 4, 197-208 (1999). PMID: 10394588
7. Small, R., Lubezky, N., Ben-Haim, M. Current controversies in the surgical management of colorectal cancer metastases to the liver. *The Israel Medical Association Journal: IMAJ* 9, 742-747 (2007). PMID: 17987765
8. Howard, J. H., Tzeng, C. W., Smith, J. K., Eckhoff, D. E., Bynon, J. S., Wang, T., Arnoletti, J. P., Heslin, M. J. Radiofrequency ablation for unresectable tumors of the liver. *The American Surgeon* 74, 594-600; discussion 600-591 (2008). PMID: 18646476
9. Shibata, T., Niinobu, T., Ogata, N., Takami, M. Microwave coagulation therapy for multiple hepatic metastases from colorectal carcinoma. *Cancer* 89, 276-284 (2000). PMID: 10918156
10. Vogl, T. J., Straub, R., Eichler, K., Sollner, O., Mack, M. G. Colorectal carcinoma metastases in liver: laser-induced interstitial thermotherapy—local tumor control rate and survival data. *Radiology* 230, 450-458 (2004). DOI: 10.1148/radiol.2302020646
11. Crocetti, L., de Baere, T., Lencioni, R. Quality improvement guidelines for radiofrequency ablation of liver tumours. *Cardiovascular and Interventional Radiology* 33, 11-17 (2010). DOI: 10.1007/s00270-009-9736-y
12. Pech, M., Mohnike, K., Wieners, G., Bialek, E., Dudeck, O., Seidensticker, M., Peters, N., Wust, P., Gademann, G., Ricke, J. Radiotherapy of liver metastases: comparison of target volumes and dose-volume histograms employing CT- or MRI-based treatment planning. *Strahlenther Onkol* 184, 256-261 (2008). PMID: 18427756
13. Dawood, O., Mahadevan, A., Goodman, K. A. Stereotactic body radiation therapy for liver metastases. *Eur J Cancer* (2009). PMID: 19773153
14. Stintzing, S., Hoffmann, R. T., Heinemann, V., Kufeld, M., Muacevic, A. Frameless single-session robotic radiosurgery of liver metastases in colorectal cancer patients. *Eur J Cancer* 46, 1026-1032 (2010). PMID: 20153959

15. Stintzing, S., Hoffmann, R. T., Heinemann, V., Kufeld, M., Rentsch, M., Muacevic, A. Radiosurgery of liver tumors: value of robotic radio-surgical device to treat liver tumors. *Ann Surg Oncol* (2010). PMID: 20574773
16. Stintzing, S., Grothe, A., Hendrich, S., Hoffmann, R. T., Heinemann, V., Rentsch, M., Fuerweger, C., Muacevic, A., Trumm, C. G. Percutaneous radiofrequency ablation (RFA) or robotic radiosurgery (RRS) for salvage treatment of colorectal liver metastases. *Acta Oncol* (2013). DOI: 10.3109/0284186X.2013.766362
17. Bruegel, M., Holzapfel, K., Gaa, J., Woertler, K., Waldt, S., Kiefer, B., Stemmer, A., Ganter, C., Rummeny, E. J. Characterization of focal liver lesions by ADC measurements using a respiratory triggered diffusion-weighted single-shot echo-planar MR imaging technique. *European Radiology* 18, 477-485 (2008). DOI: 10.1007/s00330-007-0785-9
18. Koh, D. M., Collins, D. J. Diffusion-weighted MRI in the body: applications and challenges in oncology. *AJR. American Journal of Roentgenology* 188, 1622-1635 (2007). DOI: 10.2214/AJR.06.1403
19. Hamstra, D. A., Rehemtulla, A., Ross, B. D. Diffusion magnetic resonance imaging: a biomarker for treatment response in oncology. *Journal of Clinical Oncology: Official Journal of the American Society of Clinical Oncology* 25, 4104-4109 (2007). DOI: 10.1200/JCO.2007.11.9610
20. Mannelli, L., Kim, S., Hajdu, C. H., Babb, J. S., Clark, T. W., Taouli, B. Assessment of tumor necrosis of hepatocellular carcinoma after chemoembolization: diffusion-weighted and contrast-enhanced MRI with histopathologic correlation of the explanted liver. *AJR. American Journal of Roentgenology* 193, 1044-1052 (2009). DOI: 10.2214/AJR.08.1461
21. Kamel, I. R., Bluemke, D. A., Eng, J., Liapi, E., Messersmith, W., Reyes, D. K., Geschwind, J. F. The role of functional MR imaging in the assessment of tumor response after chemoembolization in patients with hepatocellular carcinoma. *Journal of Vascular and Interventional Radiology: JVIR* 17, 505-512 (2006). DOI: 10.1097/01.RVI.0000200052.02183.92
22. Chen, C. Y., Li, C. W., Kuo, Y. T., Jaw, T. S., Wu, D. K., Jao, J. C., Hsu, J. S., Liu, G. C. Early response of hepatocellular carcinoma to transcatheter arterial chemoembolization: choline levels and MR diffusion constants—initial experience. *Radiology* 239, 448-456 (2006). DOI: 10.1148/radiol.2392042202
23. Deng, J., Miller, F. H., Rhee, T. K., Sato, K. T., Mulcahy, M. F., Kulik, L. M., Salem, R., Omary, R. A., Larson, A. C. Diffusion-weighted MR imaging for determination of hepatocellular carcinoma response to yttrium-90 radioembolization. *Journal of Vascular and Interventional Radiology: JVIR* 17, 1195-1200 (2006). DOI: 10.1097/01.RVI.0000227234.81718.EB
24. Anzidei, M., Napoli, A., Zaccagna, F., Cartocci, G., Saba, L., Menichini, G., Cavallo Marincola, B., Marotta, E., Di Mare, L., Catalano, C., Passariello, R. Liver metastases from colorectal cancer treated with conventional and antiangiogenic chemotherapy: evaluation with liver computed tomography perfusion and magnetic resonance diffusion-weighted imaging. *Journal of Computer Assisted Tomography* 35, 690-696 (2011). DOI: 10.1097/RCT.0b013e318230d905
25. Malayeri, A. A., El Khouli, R. H., Zaheer, A., Jacobs, M. A., Corona-Villalobos, C. P., Kamel, I. R., Macura, K. J. Principles and applications of diffusion-weighted imaging in cancer detection, staging, and treatment follow-up. *Radiographics: a Review Publication of the Radiological Society of North America, Inc* 31, 1773-1791 (2011). DOI: 10.1148/rg.316115515
26. World Medical Association Declaration of Helsinki: ethical principles for medical research involving human subjects. *JAMA: The Journal of the American Medical Association* 284, 3043-3045 (2000). PMID: 11122593
27. Lartigau, E., Mirabel, X., Prevost, B., Lacombe, T., Dubus, F., Sarrazin, T. Extracranial stereotactic radiotherapy: preliminary results with the CyberKnife. *Onkologie* 32, 209-215 (2009). DOI: 10.1159/000200929
28. Eisenhauer, E. A., Therasse, P., Bogaerts, J., Schwartz, L. H., Sargent, D., Ford, R., Dancey, J., Arbuck, S., Gwyther, S., Mooney, M., Rubinstein, L., Shankar, L., Dodd, L., Kaplan, R., Lacombe, D., Verweij, J. New response evaluation criteria in solid tumours: revised RECIST guideline (version 1.1). *Eur J Cancer* 45, 228-247 (2009). DOI: 10.1016/j.ejca.2008.10.026
29. Ambrosino, G., Polistina, F., Costantin, G., Francescon, P., Guglielmi, R., Zanco, P., Casamassima, F., Febbraro, A., Gerunda, G., Lumachi, F. Image-guided robotic stereotactic radiosurgery for unresectable liver metastases: preliminary results. *Anticancer Research* 29, 3381-3384 (2009). PMID: 19661360
30. Goyal, K., Einstein, D., Yao, M., Kunos, C., Barton, F., Singh, D., Siegel, C., Stulberg, J., Sanabria, J. Cyberknife stereotactic body radiation therapy for nonresectable tumors of the liver: preliminary results. *HPB Surgery: A World Journal of Hepatic, Pancreatic and Biliary Surgery* 2010 (2010). DOI: 10.1155/2010/309780
31. Dewas, S., Bibault, J. E., Mirabel, X., Fumagalli, I., Kramar, A., Jarraya, H., Lacombe, T., Dewas-Vautravers, C., Lartigau, E. Prognostic factors affecting local control of hepatic tumors treated by Stereotactic Body Radiation Therapy. *Radiat Oncol* 7, 166 (2012). DOI: 10.1186/1748-717X-7-166
32. Nishino, M., Jagannathan, J. P., Ramaiya, N. H., Van den Abbeele, A. D. Revised RECIST guideline version 1.1: What oncologists want to know and what radiologists need to know. *AJR. American Journal of Roentgenology* 195, 281-289 (2010). DOI: 10.2214/AJR.09.4110
33. Kamel, I. R., Bluemke, D. A. Magnetic resonance imaging of the liver: assessing response to treatment. *Topics in Magnetic Resonance Imaging: TMRI* 13, 191-200 (2002). PMID: 12357082
34. Galban, C. J., Chenevert, T. L., Meyer, C. R., Tsiens, C., Lawrence, T. S., Hamstra, D. A., Junck, L., Sundgren, P. C., Johnson, T. D., Ross, D. J., Rehemtulla, A., Ross, B. D. The parametric response map is an imaging biomarker for early cancer treatment outcome. *Nature Medicine* 15, 572-576 (2009). DOI: 10.1038/nm.1919
35. Dromain, C., de Baere, T., Elias, D., Kuoch, V., Ducreux, M., Boige, V., Petrow, P., Roche, A., Sigal, R. Hepatic tumors treated with percutaneous radio-frequency ablation: CT and MR imaging follow-up. *Radiology* 223, 255-262 (2002). PMID: 11930075
36. Kalb, B., Chamsuddin, A., Nazzal, L., Sharma, P., Martin, D. R. Chemoembolization follow-up of hepatocellular carcinoma with MR imaging: usefulness of evaluating enhancement features on one-month posttherapy MR imaging for predicting residual disease. *Journal of Vascular and Interventional Radiology: JVIR* 21, 1396-1404 (2010). DOI: 10.1016/j.jvir.2010.05.015
37. Lim, H. K., Han, J. K. Hepatocellular carcinoma: evaluation of therapeutic response to interventional procedures. *Abdominal Imaging* 27, 168-179 (2002). PMID: 11847576
38. Guo, Y., Cai, Y. Q., Cai, Z. L., Gao, Y. G., An, N. Y., Ma, L., Mahankali, S., Gao, J. H. Differentiation of clinically benign and malignant breast lesions using diffusion-weighted imaging. *Journal of Magnetic Resonance Imaging: JMIR* 16, 172-178 (2002). DOI: 10.1002/jmri.10140
39. Sugahara, T., Korogi, Y., Kochi, M., Ikushima, I., Shigematu, Y., Hirai, T., Okuda, T., Liang, L., Ge, Y., Komohara, Y., Ushio, Y., Takahashi, M. Usefulness of diffusion-weighted MRI with echo-planar technique in the evaluation of cellularity in gliomas. *Journal of Magnetic Resonance Imaging: JMIR* 9, 53-60 (1999). PMID: 10030650
40. Lang, P., Wendland, M. F., Saeed, M., Gindele, A., Rosenau, W., Mathur, A., Gooding, C. A., Genant, H. K. Osteogenic sarcoma: non-invasive in vivo assessment of tumor necrosis with diffusion-weighted MR imaging. *Radiology* 206, 227-235 (1998). PMID: 9423677
41. Schmid-Tannwald, C., Oto, A., Reiser, M. F., Zech, C. J. Diffusion-weighted MRI of the abdomen: current value in clinical routine.

Journal of Magnetic Resonance Imaging: JMRI 37, 35-47 (2013).
DOI: 10.1002/jmri.23643

42. Eccles, C. L., Haider, E. A., Haider, M. A., Fung, S., Lockwood, G., Dawson, L. A. Change in diffusion weighted MRI during liver cancer radiotherapy: preliminary observations. *Acta Oncol* 48, 1034-1043 (2009). DOI: 10.1080/02841860903099972
43. Wybranski, C., Zeile, M., Lowenthal, D., Fischbach, F., Pech, M., Rohl, F. W., Gademann, G., Ricke, J., Dudeck, O. Value of diffusion

weighted MR imaging as an early surrogate parameter for evaluation of tumor response to high-dose-rate brachytherapy of colorectal liver metastases. *Radiat Oncol* 6, 43 (2011). DOI: 10.1186/1748-717X-6-43

44. Lanciano, R., Lamond, J., Yang, J., Feng, J., Arrigo, S., Good, M., Brady, L. Stereotactic body radiation therapy for patients with heavily pretreated liver metastases and liver tumors. *Frontiers in Oncology* 2, 23 (2012). DOI: 10.3389/fonc.2012.00023

Received: July 14, 2013; Revised: November 15, 2013;

Accepted: November 22, 2013

